Laboratory simulation of western boundary currents over shelf topography and of their extensions

NTNU Coriolis
NTNU Coriolis Shelf Topography

EC contract no. 261520

Status: draft
Date: Aug 2008

Infrastructure	NTNU Coriolis		
Project	Laboratory simulation of western boundary currents over shelf topography and of their extensions		
Campaign	HyIII-NTNU-15		
Title	NTNU Coriolis Shelf Topography		
Lead Author	Stefano Pierini	**Email**	stefano.pierini@uniparthenope.it
Contributors	Pierpaolo Falco	**Email**	pierpaolo.falco@uniparthenope.it
Date Campaign Start	30/08/2008	**Date Campaign End**	20/09/2008
Date Final Completion			

Contents:

1. Scientific aim and background:

1.1 Modeling Western Boundary Currents in rotating tanks

the oceanographic relevance of the problem and the sliced cylinder and cone models Western boundary currents (WBCs) are fundamental features of the large-scale wind-driven oceancirculation. In the subtropical (subpolar) gyres they are narrow and intense poleward (equatorward) currents (e.g., the Gulf Stream in the North Atlantic, the Kuroshio and Oyashio in the North Pacific, the East Australian Current in the South Pacific, etc.) that play a fundamental role in the global climate, as they provide a substantial fraction of the oceanic meridional heat transport. Moreover, their peculiar geographical structure can have important implications on the climate of vast areas (as is the case, for instance, of the northern Gulf Stream branch of warm surface waters that flows north of the British islands, that contributes to make surface temperatures in North-Western Europe significantly higher than those typical of other regions at the same latitude). Complex mechanisms involving the wind-driven and thermohaline circulation and water mass transformation, and related to the current global warming, might induce a weakening of such northward heat transport, with possible dramatic changes in the climate of North-Western Europe (e.g. Rahmstorf 1997; 1999). This is to stress how important it is to improve our understanding of the functioning of WBCs. In the last few decades numerical simulations have almost always complemented analytical treatments in the investigation and interpretation of basic mechanisms of physical oceanography; nonetheless, a small but significant amount of experimental simulations based on the use of rotating basins and the principle of dynamic similarity have been carried out as well, and in this context WBCs have been analyzed in several cases. The main approach is based on the so-called sliced cylinder model (e.g., Pedlosky and Greenspan1967; Beardsley and Robbins 1975; Griffiths and Kiss 1999), in which a homogeneous fluid contained in a cylinder with a planar sloping bottom (that introduces an equivalent topographic beta-effect) is driven by a rotating upper lid. A generalization of this model that takes into account the effect of sloping sidewalls is known as the sliced cone model (Griffiths and Veronis 1997). These laboratory models are, in fact, conceived to simulate an idealized subtropical gyre, of which the WBC is only an important part of the flow: this requires a basin-wide surface forcing, and the resulting zonal extension of the WBC is, consequently, of only a few cm width (also because of the relative smallness of the rotating tanks used, usually of about 1 m in diameter). Moreover, the WBCs thus obtained are in a linear or moderately nonlinear regime. On the other hand, it is well known that real WBCs in the world's oceans are strongly nonlinear (e.g. Pedlosky 1996). It appeared therefore worth considering alternative experimental setups in large rotating basins that would have allowed one to investigate aspects that had not been addressed in the laboratory models mentioned above, namely: (i) the behavior of WBCs in a parameter range in which nonlinear effects are as strong as in real oceans; (ii) the production of zonal widths of the WBCs that are much larger than a few cm, so as to be able to resolve adequately the zonal profile of the alongshore velocity.

1.2 An innovative experimental setup used at SINTEF in 2003

The laboratory study performed at SINTEF in 2003 (Contract HPRI-CT-1999-00060) by Pierini et al.(2008) has met these two requirements since, thanks to the large dimension of the basin used, it has dealt with wide and strongly nonlinear WBCs. The basic idea (inspired by the companion laboratory study of topographic Rossby normal modes of Pierini et al. 1999, 2002, previously carried out at Coriolis of LEGICNRS in Grenoble) is that, assumed that the effect of the wind in the WBC region is negligible (e.g.,Pedlosky 1987), then if only the zonal structure of a WBC (and not also the whole gyre) is to be investigated, the return Sverdrup flow generated by the wind in the oceanic interior can be substituted by a remote mechanical production of a flow provided by the motion of a piston, in the absence of any surface stress. This was achieved in the 5 m diameter rotating basin at SINTEF, in Trondheim (NTNU) by using two parallel rectangular channels separated by an island and linked by two curved connections (Fig. 1.2.1). In the first channel, a piston is forced at a constant speed up ranging from 5 to 30 mm/s over a distance of 2.5 m, producing a virtually un-sheared current at the entrance of the second channel. In the latter, a linear reduction of the water depth provides the topographic beta effect that is necessary for the development of the westward intensification. Nearly steady currents are obtained and measured photogrammetrically over a region (S) of about 1 m2. In all the experiments performed, an appropriate horizontal Reynolds number (Re=ε/E, where ε and E are dimensionless numbers measuring the importance of nonlinearity and lateral friction, respectively) is Re>>1. The zonal profile of the meridional velocity is always found to have (away from the viscousboundary layer) a nearly exponential structure typical of inertial WBCs, whose width agrees well with the classical inertial boundary-layer length scale δI. A control experiment (with up=10 mm/s) is analyzed in detail: it has the same ε as the Gulf Stream (GS) but a much smaller E. This implies that the laboratory flow is expected to be geometrically similar to the GS outside the viscous boundary layer, but to differ within it. In order to assess the effect of such a departure from dynamic similarity, a mathematical shallow water model is used: this has allowed us to simulatenumerically a flow that is fully dynamically similar to the GS. The comparison between the profile thus obtained numerically and the one obtained experimentally shows that they are indeed virtually coincident outside the viscous boundary layer, except for a small offset that tends to vanish as Re→∞. Moreover, additional sensitivity experiments in which the piston speed, the rotation rate of the basin, the topographic beta effect and the width of the main channel are varied, provide further information on the zonal structure of WBCs.

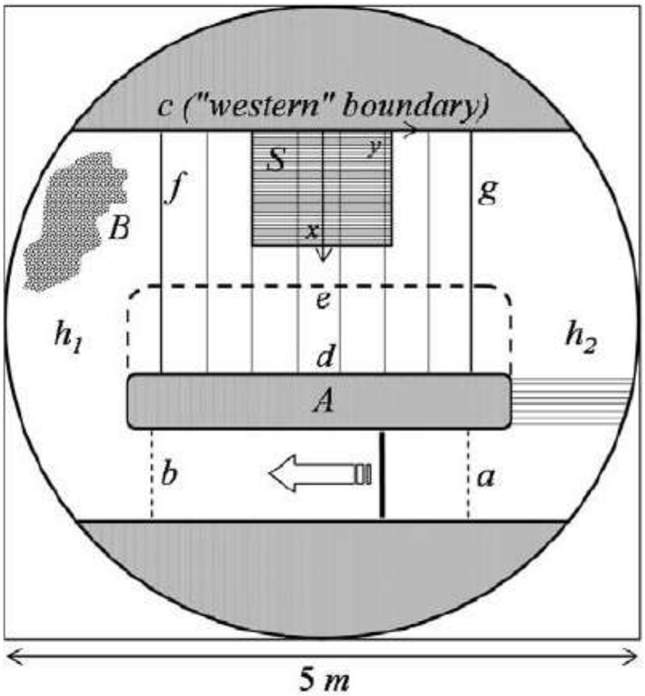

diameter of the tank:	5 m
distance (from *a* to *b*) covered by the paddle:	2.5 m
length of the paddle:	0.69 m
width of the paddle:	2 cm
width of the paddle channel:	0.7 m
length of the "island" *A*:	3.05 m
distance between *c* and *d*:	1.9 m
distance between *c* and *e*:	1.2 m
length of the bottom slope (from *f* to *g*):	2.4 m
dimension of the area *S* covered by the photogrammetry:	1.1 m x 0.90 m
maximum water depth (h_1):	40 cm
minimum water depth (h_2):	15/17/27.5 cm

Figure 1.1 The setup previously used to model western boundary currents at SINTEF (from Pierini et al. 2008).

1.3 The new experiments performed at SINTEF in September 2008

Despite the success in modeling WBCs, several important dynamical aspects have not been considered. In the new project carried out at SINTEF in September 2008 we have extended that laboratory study in order to analyze further, relevant dynamical features of WBCs according to the future developments outlined by Pierini et al. (2008) in their concluding remarks. This has required modifications in the setup, as shown in Fig. 1.2 and as discussed below.

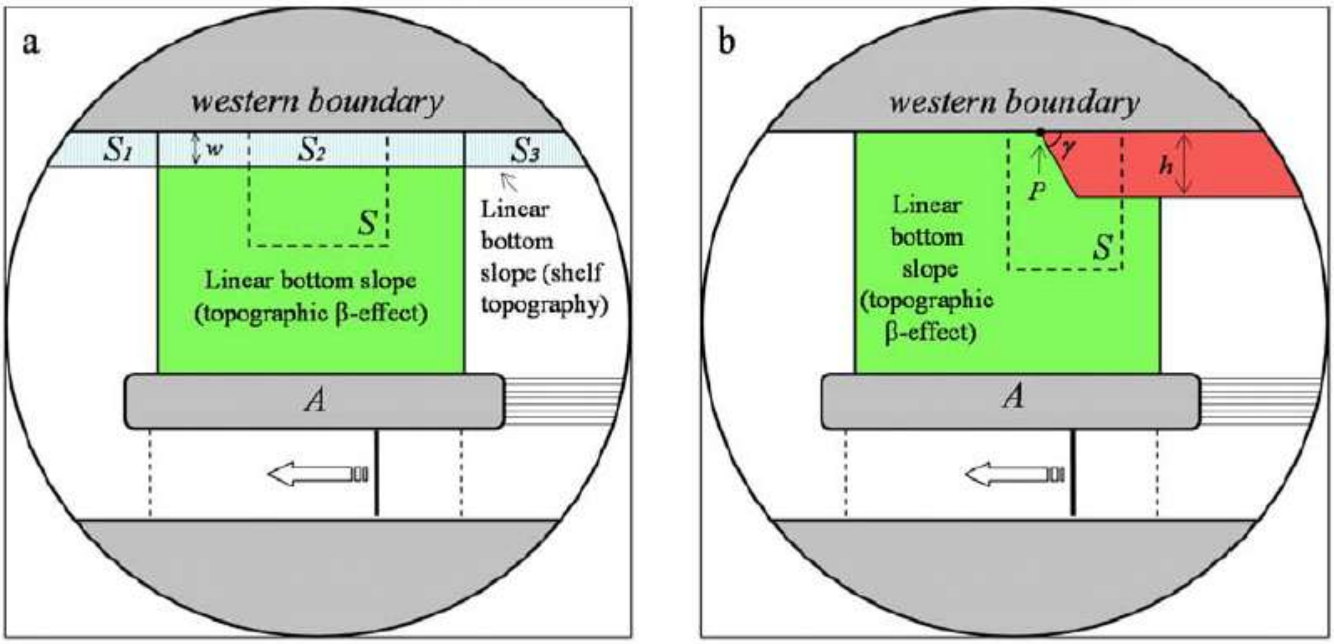

Figure 1.2 The modifications of the experimental setup considered in this project.

1.3.1 Modelling weakly nonlinear western boundary currents

The most innovative results of the study of Pierini et al. (2008), i.e. the possibility of producing inertial WBCs as strongly nonlinear as the real oceanic counterparts (while in classical simulations with sliced cylinder/cone setups the flows could only be weakly nonlinear) was strictly related to the large dimension of the Coriolis rotating basin of SINTEF. In fact, the flow generated by the piston that gave rise to the WBCs could have a sufficiently large transport thanks both to the large width (70 cm) and speed (from 5 to 30 mm/s) of the piston. Curiously enough, while with the more classical setup it was impossible to achieve a realistic degree of nonlinearity, in the experiments of 2003 it was impossible to achieve an unrealistically low degree of nonlinearity! This is because, for a fixed width of the piston channel of 70 cm, a very weak WBC could be obtained only with a very small speed of the piston; however, there was a lower limit of 5 mm/s, because below that threshold the mechanical apparatus that generated the piston motion could not have a perfectly constant speed. However, the interest in producing weak WBCs, such as linear or weakly nonlinear Munk-type flows, lies in the possibility of comparing the experimental results with analytical solutions, that are available in such cases (Pedlosky 1987, 1996). This in turn would allow one to obtain a valuable experimental validation of those theories, which, at the best of our knowledge, has never been done before. The simulation of weak WBCs was now possible thanks to an improved mechanical apparatus that impressed to the piston a perfectly constant movement with a speed as low as 0.5 mm/s! During the first week, runs with very small paddle speeds were carried out. A preliminary presentation of the obtained results is given in section 3.1.

1.3.2 Modelling western boundary currents over shelf topography

It is well known that the continental shelf topography has a relevant effect on the structure of WBCs in the vicinity of the coast, so that, in the context of laboratory simulations, the sliced cylinder cone was extended to include a sloping side boundary in the sliced cone model (see section 1.1). A clear sign of the effect of the coastal topography on the structure of the Gulf Stream before detachment is revealed by the in situ measurements of Rossby and Zhang (2001), who showed that the Gulf Stream has a stream-averaged velocity profile with a double-exponential pattern, in which the maximum velocity is located over the edge of the continental slope. Pierini et al. (2008) found that the velocity profile of their reference experiment agrees well with the outer exponential found by Rossby and Zhang (2001) but, of course, the inner exponential, that lies over shoaling water in the real ocean, is not present in their laboratory simulation performed without sloping boundary. In order to overcome this limitation, in the second week of the experiments two different linear bottom slopes along the “western” wall were included (see Fig. 1.3.1a). A preliminary presentation of the obtained results is given in section 3.2.

1.3.3 Modelling western boundary current extensions

A fundamental dynamical aspect of a WBC is its “extension”, i.e. the free jet state reached after its separation from the coast. Several theories have been proposed to explain this phenomenon: a WBC separates from the coast at the latitude where the mean wind stress curl vanishes and/or through mechanisms such as vorticity crisis and adverse pressure gradients (the latter mechanism was studied in rotating tank experiments by Baines and Hughes, 1996). Strange enough, the role of the coastal morphology in contributing to the separation does not appear to have received the attention it deserves. As far as the Kuroshio Extension is concerned, the role played by the coastline of Japan in determining the character and low-frequency variability of the Kuroshio Extension (KE) was recognized to be crucial in recent model studies (Pierini 2006a,b, 2008, Pierini et al. 2008). In particular, it was shown (Pierini 2006a, 2008) that the decadal chaotic relaxation oscillation produced by the model (and found to be in surprisingly good agreement with the observed variability of the KE in the period 1992-2004 as inferred from altimeter data by Qiu and Chen, 2005) completely disappears if the coastal geometry of southern Japan is substituted by a meridional coast. On the other hand, the Gulf Stream separates at Cape Hatteras where the coast bends to the north-west, and continues its path to the north-east. So the coastal shape may well have a profound effect on the separation mechanism. Thus, it appears of great interest to begin addressing the role of the shape of the western boundary in the separation of WBC extensions in rotating tank experiments. From the end of the second week onward the introduction of "capes" along the western wall has allowed us to test the role of the coastal morphology in the separation process. A preliminary presentation of the obtained results is given in section 3.3.

References

Baines, P.G., Hughes, R.L ., 1996. Western boundary current separation: inferences from a laboratory experiment. *J. Phys. Oceanogr* ., 26, 2576-2588.

Beardsley, R.C., Robbins, K., 1975. The 'sliced-cylinder' laboratory model of the wind-driven ocean circulation. Part 1. Steady forcing and topographic Rossby wave instability. *J. Fluid. Mech*., 69, 27-40.

Griffiths, R.W., Kiss, A.E., 1999. Flow regimes in a wide 'sliced-cylinder' model of homogeneous -planecirculation. *J. Fluid Mech*., 399, 205-236.

Griffiths, R.W., Veronis, G., 1997. A laboratory study of the effects of a sloping side boundary on wind-driven circulation in a homogeneous ocean model.

J. Marine Res., 55, 1103-1126.

Pedlosky, J., 1987. *Geophysical Fluid Dynamics*. Springer Verlag, 710 pp.

Pedlosky, J., 1996. *Ocean Circulation Theory*. Springer, 453 pp.

Pedlosky, J., Greenspan, H.P., 1967. A simple laboratory model for the oceanic circulation. *J. Fluid. Mech*., 27, 291-304.

Pierini, S., 1996. Topographic Rossby modes in the Strait of Sicily. *J. Geophys. Res*., 101, 6429-6440.

Pierini, S., 2006a. A Kuroshio Extension system model study: decadal chaotic self-sustained oscillations. *J. Phys.Oceanogr.*, 36, 1605-1625.

Pierini, S., 2006b. Seasonal and interannual variability of the North Pacific Ocean: modeling results and their validation through altimeter data. In Proceedings of the *ESA-CNES* Symposium: "*15 Years of Progress in Radar Altimetry*". European Space Agency (ISBN/ISSN: 92-9092-925-1/1609-042X), Vol. SP-614.

Pierini, S., 2008. On the crucial role of basin geometry in double-gyre models of the Kuroshio Extension. *J. Phys.Oceanogr.*, 38, 1327-1333.

Pierini, S., Dijkstra, H.A., Riccio, A., 2008. A nonlinear theory of the Kuroshio Extension bimodality. Submitted.

Pierini, S., Fincham, A., Renouard, D., D'Ambrosio, R., Didelle, H., 1999. Topographic Rossby normal modes simulated in the "Coriolis" rotating tank and by means of a mathematical model. In

Proceedings of the *HYDRALAB Workshop (Hannover): "Experimental research and synergy effects with mathematical models"* (K.U. Evers, J. Grüne and A. van Os Editors), 171-180.
Pierini, S., Fincham, A., Renouard, D., D'Ambrosio, R., Didelle, H., 2002. Laboratory modeling of topographic Rossby normal modes. *Dyn. Atmos. Oceans,* 35, 205-225.

Pierini, S., Malvestuto, V., Siena, G., McClimans, T. A., Løvås S. M., 2008. A laboratory study of the zonal structure of western boundary currents. *J. Phys. Oceanogr.*, 38, 1073-1090.

Qiu, B., Chen, S., 2005. Variability of the Kuroshio Extension jet, recirculation gyre, and mesoscale eddies on decadal time scales. *J. Phys. Oceanogr.*, 35, 2090-2103.
Rahmstorf, S., 1997. Risk of sea-change in the Atlantic. *Nature*, *388*, 825-826.

Rahmstorf, S, 1999. Shifting seas in the greenhouse? *Nature*, 399, 523-524.

Rossby, T., Zhang, H.M., 2001. The near-surface velocity and potential vorticity structure of the Gulf Stream. *J. Mar.Res*., 59, 949-975.

2. User-Project Achievements and difficulties encountered:

Part (1) of the study has required a new mechanical apparatus that has allowed for speeds of the piston generating the flow as low as 0.5 mm/s, part (2) has required the introduction of sloping sidewalls, while, for part (3), four different obstacles have been added along the western boundary in order to analyze coastal detachment. In all cases the photogrammetry system, the generation of dye streams and the digital visual recording of all the experiments have provided a detailed and satisfactory data set suitable for the future scientific analyses.

No difficulties have been encountered in the experimental activity; the local assistance was so efficient and the research team was so well organized that a very large number (65) of experiments could be carried out in the three available weeks. The only minor problem concerns the retrieving of the velocity vectors from the digital images taken from the photogrammetry system, that failed to work in some cases -near the wall- during the real-time data processing. However, that problem does not affect the validity of the measurements but only the post-processing of the bitmap images, which were always taken in the correct way (the personnel responsible for the measuring system will soon find the solution of the problem).

3. Highlights important research results:

A preliminary analysis of the obtained results indicates that all the scientific aims have been achieved. The transition from highly nonlinear western boundary currents to weakly nonlinear ones is now evidenced in the measurements, so that an unprecedented coverage on the range of nonlinearity for WBCs is now available in terms of experimental data. The simulation of the effect of sloping sidewalls has been properly carried out, and those data will be analyzed in detail on the basis of theoretical arguments.

Perhaps the most interesting results concern the third part of the study. While for weak WBCs the current follows the coast even past the cape, for strong WBCs a free jet is found to detach from the coast. Thus, it was clearly shown that WBC detachment can be produced by a discontinuity of the coastline. Moreover, the transition between these two very different behaviors is marked by a case corresponding to the experiment of Pierini et al. (2008) that was found to be virtually dynamically similar to the Gulf Stream. Thus, insofar as this simple analysis represents a rough representation of the North Atlantic WBC, this result would seem to suggest that a sufficient weakening of the Gulf Stream intensity would prevent flow separation past Cape Hatteras. Naturally, a real oceanic WBC is far more complex than such a simple mechanistic dynamical model, but nonetheless, these results can constitute the basis for more realistic and significant laboratory experiments that could be performed in the future.

4. Publications, reports from the project:

We expect to publish a paper in the Journal of Physical Oceanography, i.e. in the same journal where Pierini et al. (2008) published their results obtained in the previous project and that constitute the basis for the new experiments. Moreover, a communication will be submitted to session NP6.2 (Geophysical Fluid Dynamics Laboratory Experiments) of the next European Geosciences Union that will be held in Vienna on 19-24 April 2009.

5. Description:

5.1. Description:

In this section some elements of the preliminary analysis obtained for the three sets of experiments discussed in sections 1.3.1-2-3 will be briefly presented

Simulation of weakly nonlinear western boundary currents

The first week was devoted to model weak western boundary currents (see section 1.3.1). The photogrammetry was located and calibrated exactly as in Pierini et al. (2008) according to Fig. 1.1. 15 experiments have been performed by varying the rotation angular velocity T_{rot} and the paddle speed u_{paddle}. Fig. 5.1.1 shows an example of zonal velocity profiles of weakly nonlinear western boundary currents. The red line corresponds to a strongly nonlinear WBC denoted as Exp. N by Pierini et al. (2008) and produced by u_{paddle} = 10 mm/s with T_{rot} = 60 s. The other lines show how the profile is modified as the intensity of the WBC decreases. It is immediately clear that not only the amplitude decreases, but also the width of the WBC decreases notably, this being indicative of a transition to a more and more weak degree of nonlinearity. The weakest profiles corresponding to 1 and 0.5 mm/s show qualitatively a Munk-like profile, and this will be verified quantitatively in the future analysis.

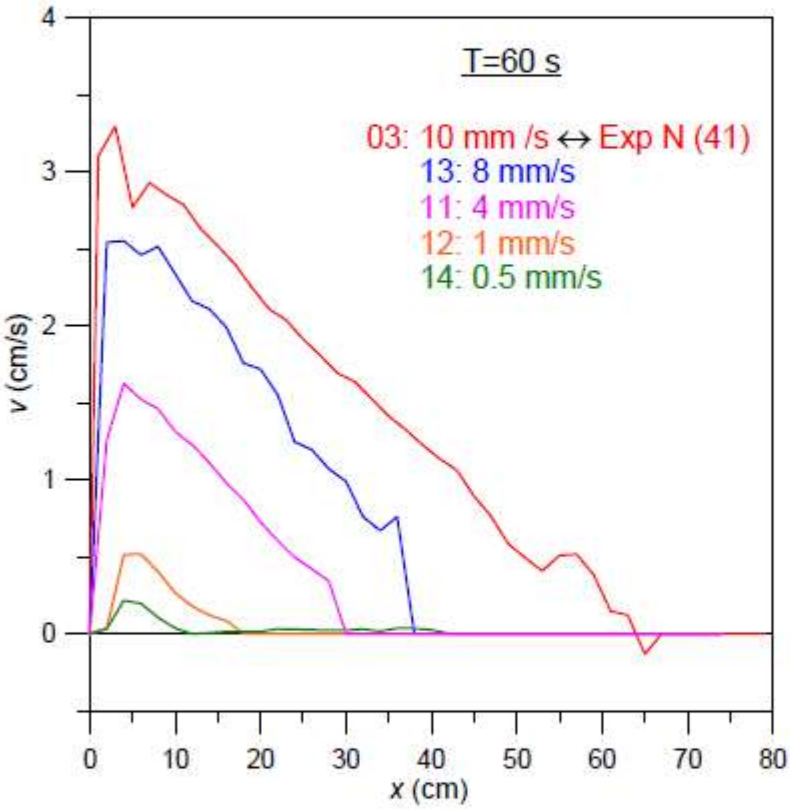

Figure 5.1.1 Example of zonal profiles of the merifional velocity of weakly nonlinear western boundary currents.

Simulation of western boundary currents over shelf topography

The second week was devoted to model western boundary currents over shelf topography (see section 1.3.2). Two different slopes have been considered: “slope1” and “slope2” shown in Fig. 5.1.2a-b respectively (two more views of the topography are reported in Fig. 3.2.2): the first has a 27° slope while the second has a 20° slope. 18 experiments have been performed by varying T_{rot} and u_{paddle}. Fig. 5.1.3 shows an example of the obtained results. The red histograms give the zonal profile of the meridional velocity of the western boundary current with u_{paddle} = 8 mm/s and T_{rot} = 30 s against a vertical wall, while the blue and green histograms give the same WBC flowing over slope1 and slope2, respectively. These results will be analyzed in detail on the basis of theoretical arguments.

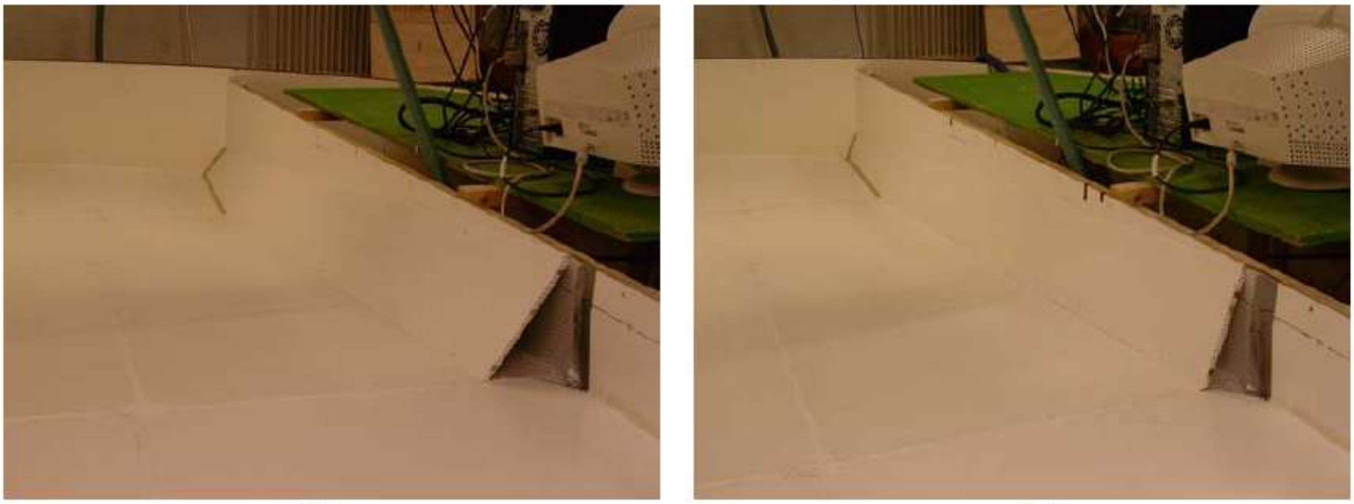

(a) (b)

Figure 5.1.2 slope1 (a) and slope2 (b).

(a) (b)

Figure 5.1.3 (a): frontal view of the slope. (b): view of the western boundary in the tank filled with water.

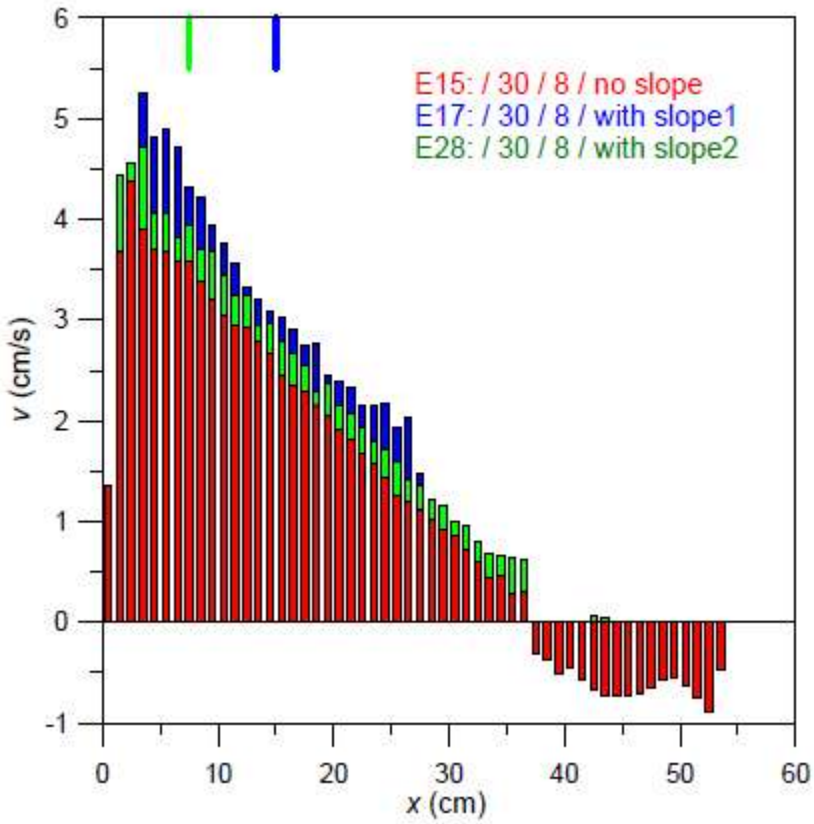

Figure 5.1.4 Example of zonal profiles of the meridional velocity of western boundary currents against a vertical wall (red histograms) and over sloping sidewalls (green and blue histograms). The blue and green vertical segments on top indicate the zonal extension of the coastal topography.

Simulation of western boundary current extensions

The third and final week was devoted to model western boundary currents that impinge against an inclined barrier (see section 1.3.3). Four different "capes" have been introduced: cape1, cape2 cape3 (see Fig. 5.1.5 and 5.1.6) and cape1-south (Fig. 5.1.7). The first three barriers present an inclined wall that forms an angle with the "latitudinal" direction of 45°, 30° and 15°, respectively, and were located along the western boundary starting from a distance of 40 cm from its center (Fig. 5.1.5), which corresponds to the origin of the axis (see Fig. 1.2). The fourth obstacle, cape1-south, is like cape1 but shifted 10 cm to the south.

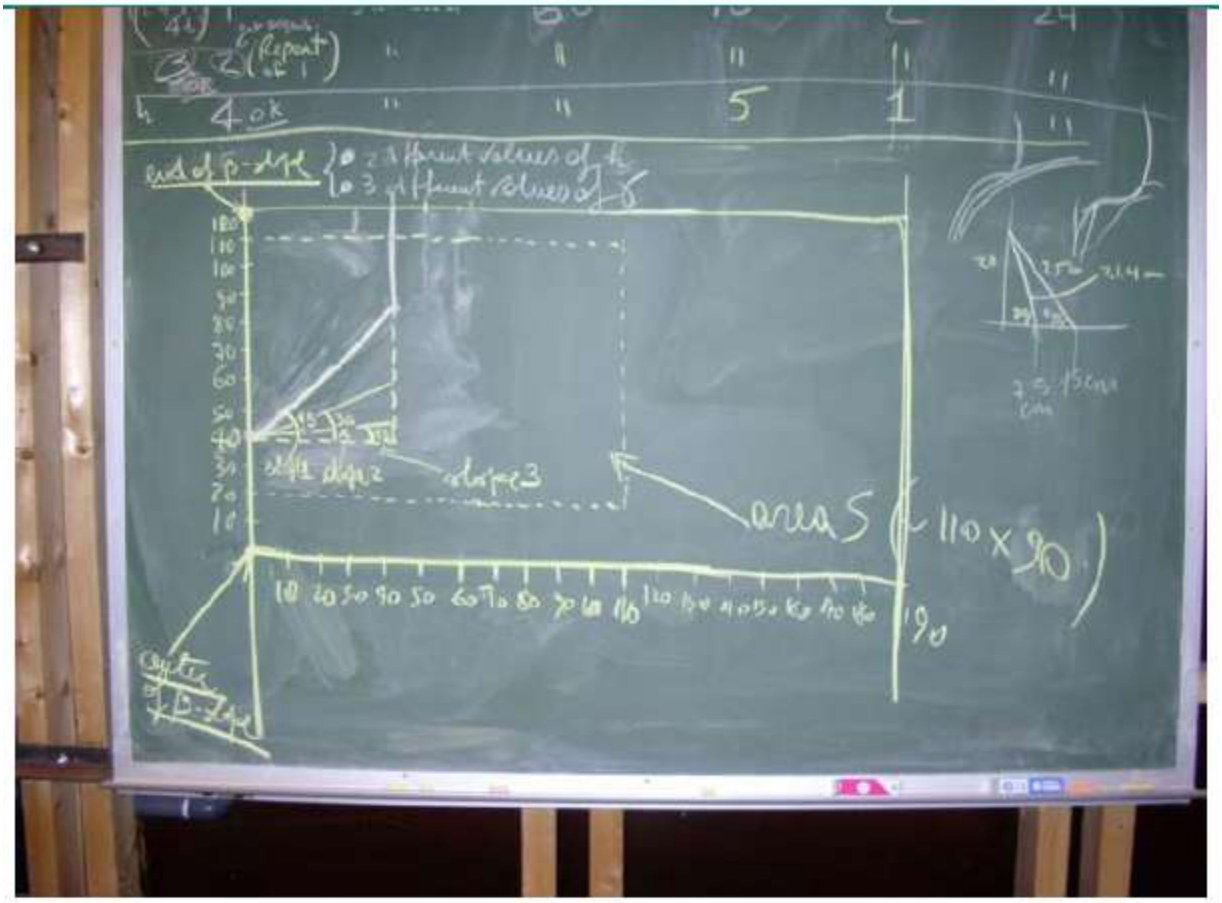

Figure 5.1.5 Sketch over the blackboard of the Coriolis laboratory of cape1, cape2 and cape3 (here“slope1-2-3” should be read “cape1-2-3”). The area S covered by the photogrammetry is also reported.

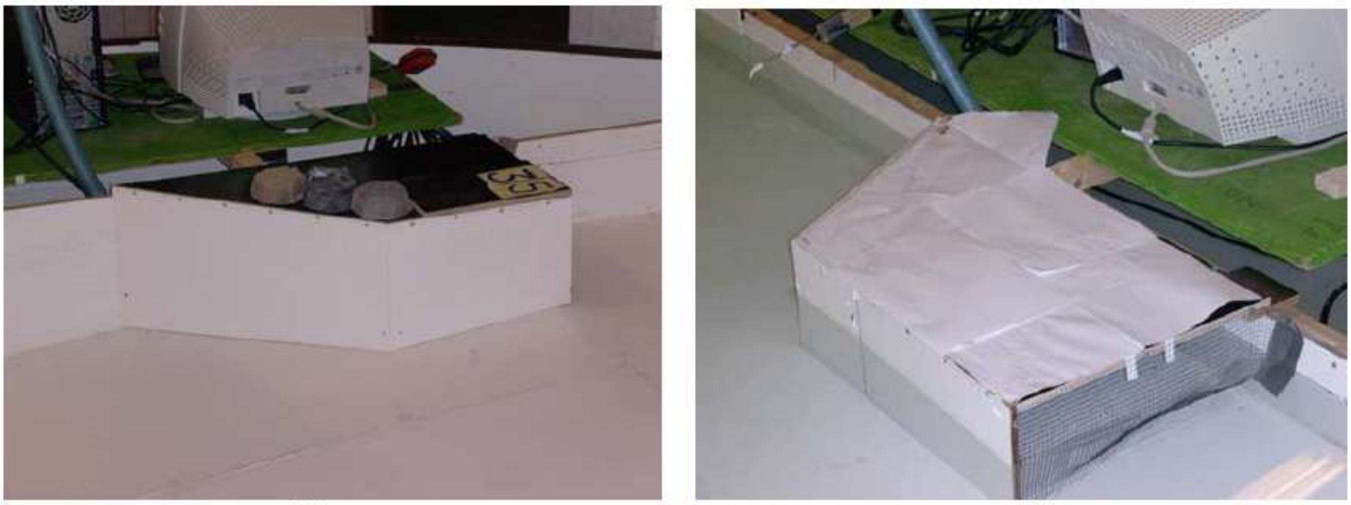

(a) (b)

Figure 5.1.6 Photos of cape1 (a) and cape2 (b).

(a) (b)

Figure 5.1.7 Photos of cape1-south. In (b) the apparatus used to produce the dye stream is visible.

For these experiments the photogrammetry system was moved from the classical location to a new one, so that the area S (see Fig. 5.1.5) could now cover the current flowing along the capes. Of course, a new calibration procedure has been necessary. 32 experiments have been performed by varying Trot and upaddle. The most interesting result is shown in Fig. 5.1.8, where the path of the WBC is evidenced in 6 different experiments by a dye stream produced by the apparatus shown Fig. 5.1.8b (the quantitative analysis based on the velocity vectors retrieved by means of the photogrammetry technique will be carried out in the near future).

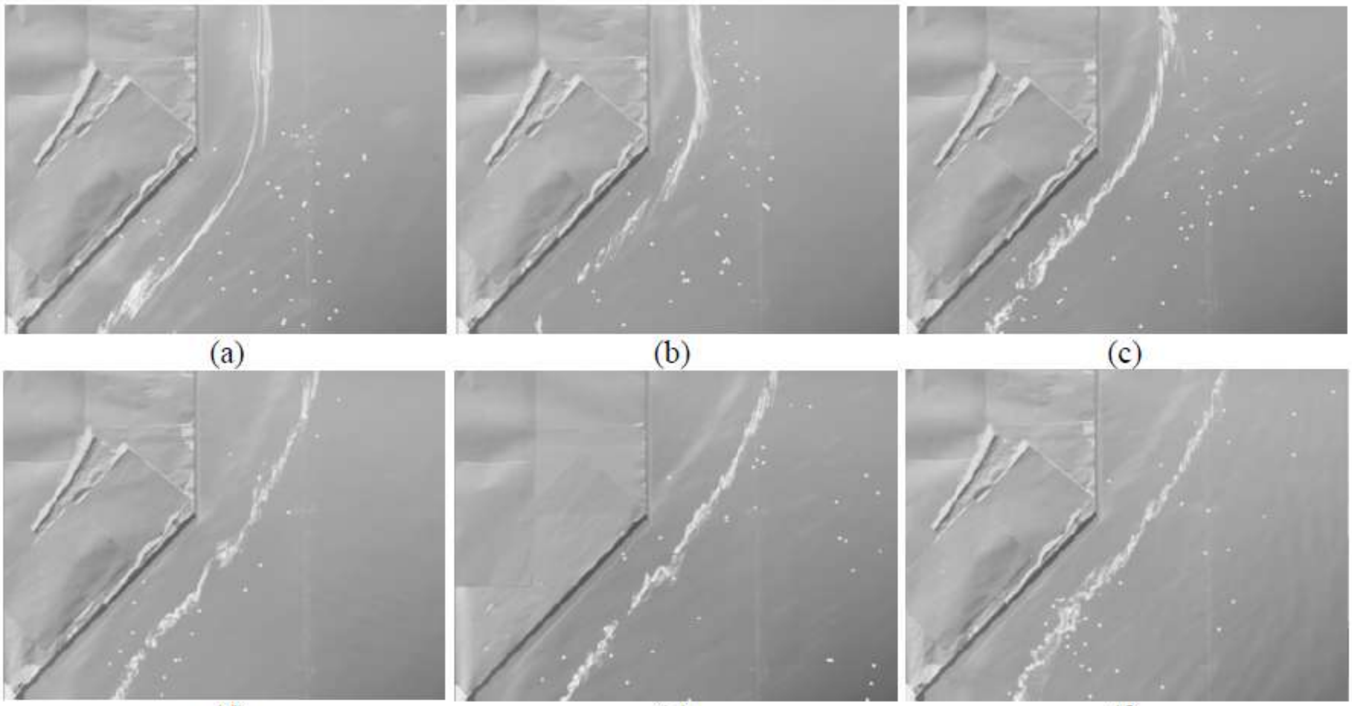

(a) (b) (c)

(d) (e) (f)

Figure 5.1.8 Images taken after spinup in experiments 63 (a), 62 (b), 61 (c), 65 (d), 59 (e), 64 (f). They all refer to runs with $T_{rot} = 30$ s and with the obstacle “cape1-south. The respecitve paddle speeds are: $u_{paddle} = 2.5, 5, 10, 15, 20, 30$ mm/s. The flow of case (c) was found to be nearly dynamically similar to the Gulf Stream by Pierini et al. (2008).

While for weak WBCs (u_{paddle} = 2.5, 5 mm/s, fig. 5.1.8a,b) the current follows the coast even past the cape, for strong WBCs (u_{paddle} = 15, 20, 30 mm/s, fig. 5.1.8d,e,f) a free jet detaches from the coast past the cape following a direction roughly parallel to the inclined barrier. Thus, this sensitivity experiment shows that a sufficiently strong WBC can detach from the coast simply as a consequence of a discontinuity of the coastline of the kind adopted here. Moreover, it is very important to notice that the transition between these two very different behaviors is marked by the case u_{paddle} = 10 mm/s (Fig. 5.1.8c): but this corresponds exactly to the Exp. B of Pierini et al. (2008), which was found to be virtually dynamically similar to the Gulf Stream. Thus, insofar as this simple analysis represents a rough representation of the North Atlantic WBC, this result would seem to suggest that a weakening of the Gulf Stream intensity by a mere factor of 2 or so could have the effect of preventing flow separation past Cape Hatteras. Naturally, a real oceanic WBC is a far more complex dynamical phenomenon than the mechanistic dynamics depicted by these simple simulations, but nonetheless, the latter can constitute the basis for more realistic and significant laboratory experiments that could be performed in the future.

5.2. Definition of the coordinate systems used:

The coordinate system used is shown in Fig. 1.1.

5.3. Instruments used:

5.4. Definition of time origin and instrument synchronisation:

The time origin corresponds to the moment when the piston starts moving. The time Δt after which the data acquisition begins depends on the experiment.

6. Definition and notation of the experimental parameters:

6.1. Fixed parameters:

See Figure 1.1 for a list of fixed parameters.

6.2. Variable independent parameters:

Notation	Name	Unit	Definition	Remarks

Table 6.2.1

6.3. Derived parameters and relevant non-dimensional numbers:

Notation	Name	Unit	Definition	Remarks

Table 6.3.1

7. Description of the experimental campaign, list of experiments:

Experiment Name	Experiment Date	Remarks

Table 7.1

8. Data processing:

Every run has led to the creation of bitmap images that have then to be processed with the photogrammetry software in order to produce the ASCII files with the velocity field. Fig. 8.1 gives an example of such a field, that includes all the velocity vectors obtained during a whole experiment.

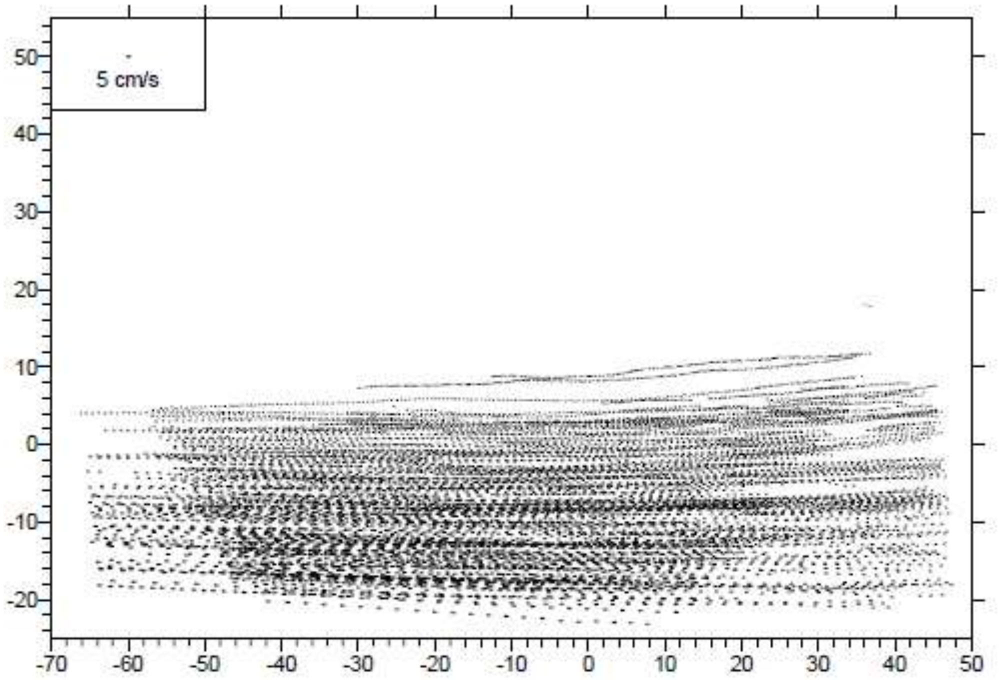

Figure 8.1 Example of the velocity vectors obtained during a whole experiment.

From these data, and through an appropriate spatial and temporal averaging procedure (see Pierini et al. 2008), the zonal profiles of the meridional velocity are obtained. These velocity data have been (and will be) processed through a software developed by the research team. The SURFER and GRAPHER graphic package of the Golden Software are used for the graphical images.

The complete list of the experiments performed is listed in the tables below. Note that all the comments are in Italian, but the different parameter values can be easily identified.

Exp. - date	T_{rot} (s)	u_{paddle} (mm/s)	fps	Data acquisition settings	Duration of data acq. (s)	Duration of run (s)	Diff. in durations (s)	comments
I week:								
01 - 020908	60 (6.65)	10	2	2 / 500 / 1 / 1	250	268		Corrisponde all'**Exp. N** (ex run 41). All'inizio l'acquisizione non è partita a causa di problemi di memoria del computer. Poi ha iniziato a funzionare, ma soltanto alla fine del run. Ottima distribuzione delle boe.
02 - 020908	"	"	"	"	"	"		L'acquisizione non è partita proprio. Si decide di riavviare il computer ogni volta che si inizia un nuovo run. Inoltre ora si passa da 500 a 450 immagini. Comunque c'è la registrazione.
03 - 020908	"	"	"	2 / 450 / 1 / 1	225	"		Finalmente è tutto ok.
04 - 020908	60	5	1	1 / 450 / 1 / 1	450	536		Ok.
05 - 020908	60	2	1/2	1 / 1 / 450 / 2	900	1340		Ok.
06 - 030908	30 (16.35)	5	1	1 / 450 / 1 / 1	450	536	-86	Corrisponde all'**Exp. A** (ex run 50). Ottimo. Avvio dell'acquisizione 90 s dopo l'avvio del paddle.
07 - 030908	30	2	1/2	1 / 1 / 700 / 2	1400	1340	+	Ottimo. **Con + l'acquisizione viene avviata contemporaneamente all'avvio del paddle (vale anche per i run successivi)**
08 - 030908	30	1	1/5	1 / 1 / 550 / 5	2750	2680	+	Ottimo.
09 - 040908	30	0.5	1/10	1 / 1 / 550 / 10	5500	5360	+	Ottimo. Si nota un allineamento delle boe lungo una linea parallela alla costa e distante da essa di qualche mm, soprattutto verso la fine della zona S (vedere registrazione, NB: si è cambiata la vel. di reg. durante il run)). Tom lo spiega come conseguenza dell'upwelling dovuto al vento provocato dalla rotazione (per velocità maggiori questo effetto è fortunatamente mascherato dalla wbc forte. Si nota anche un fortissimo clustering finale lungo la linea di stagnazione, dovuto allo spostamento offshore delle boe verso tale linea (vedere anche foto PP). Vedi esp. 14 per T=60 s.
10 - 040908	30	4	1	1 / 450 / 1 / 1	450	670	-220	Ok. Avvio dell'acquisizione – 135 s dopo l'avvio del paddle.
11 - 040908	60 (3.9!)	4	1	1 / 450 / 1 / 1	450	670	-220	Ok. Avvio dell'acquisizione – 150 s dopo l'avvio del paddle.
12 - 040908	60	1	1/5	1 / 1 / 550 / 5	2750	2680	+	Ok.
13 - 040908	60	8	2	2 / 450 / 1 / 1	225	335	-110	Ok. Avvio dell'acquisizione – 110 s dopo l'avvio del paddle.
14 - 050908	60	0.5	1/10	1 / 1 / 550 / 10	5500	5360	+	Ok. Vedere i commenti dell'esp. 09. A questa velocità di rotazione l'effetto dell'upwelling è pressochè assente! C'è stato un periodo intermedio durante il quale pochissime particelle sono presenti all'interno della zona S. Molte particelle sono state riseminate da Tom.
15 - 050908	30 (7.5)	8	2	2 / 450 / 1 / 1	225	335	-110	Ok. Avvio dell'acquisizione – 110 s dopo l'avvio del paddle.
II week:								
16 - 080908	30 (7.5)	10	2	2 / 450 / 1 / 1	225	268	-43	Ok. Esp con **SLOPE1**. Corrisponde all'EXP. B (ex run 22) ma con slope. Avvio dell'acquisizione – 40 s dopo l'avvio del paddle.
17 - 080908	30	8	2	2 / 450 / 1 / 1	225	335	-110	Ok. Esp con **SLOPE1**. Corrisponde al RUN15. Avvio dell'acquisizione – 110 s dopo l'avvio del paddle.
18 - 080908	30	4	1	1 / 450 / 1 / 1	450	670	-220	Ok. Esp con **SLOPE1**. Corrisponde al RUN10. Avvio dell'acquisizione – 140 s dopo l'avvio del paddle.
19 - 080908	30	2	1/2	1 / 1 / 700 / 2	1400	1340	+	Ok. Esp con **SLOPE1**. Corrisponde al RUN07.
20 - 080908	30	1	1/5	1 / 1 / 550 / 5	2750	2680	+	Ok. Esp con **SLOPE1**. Corrisponde al RUN08. Da questo esp. in poi si mette =0 il parametro "rotation time" su suggerimento di Ingrid.

21 - 080908	60 (3.93)	10	2	2 / 450 / 1 / 1	225	268	-43	Ok. Esp con SLOPE1. Corrisponde al RUN03. Avvio dell'acquisizione – 60 s dopo l'avvio del paddle.
22 - 090908	60	8	2	2 / 450 / 1 / 1	225	335	-110	Ok. Esp con SLOPE1. Corrisponde al RUN13. Avvio dell'acquisizione – 110 s dopo l'avvio del paddle.
23 - 090908	60	4	1	1 / 450 / 1 / 1	450	670	-220	Ok. Esp con SLOPE1. Corrisponde al RUN11. Avvio dell'acquisizione – 210 s dopo l'avvio del paddle.
24 - 090908	60	2	1/2	1 / 1 / 700 / 2	1400	1340	+	Ok. Esp con SLOPE1. Corrisponde al RUN05.
25 - 090908	60	1	1/5	1 / 1 / 550 / 5	2750	2680	+	Ok. Esp con SLOPE1. Corrisponde al RUN12.
26 - 100908	60	8	2	2 / 450 / 1 / 1	225	335	-110	Ok. Esp con SLOPE2. Corrisponde al RUN@@. Avvio dell'acquisizione – 100 s dopo l'avvio del paddle.
27 - 100908	60	2	1/2	1 / 1 / 700 / 2	1400	1340	+	Ok. Esp con SLOPE2. Corrisponde al RUN0@@
28 - 100908	30	8	2	2 / 450 / 1 / 1	225	335	-110	Ok. Esp con SLOPE2. Corrisponde al RUN@@. Avvio dell'acquisizione – 110 s dopo l'avvio del paddle.
29 - 100908	30	2	1/2	1 / 1 / 700 / 2	1400	1340	+	Ok. Esp con SLOPE2. Corrisponde al RUN0@@
30 - 100908	30	4	1	1 / 450 / 1 / 1	450	670	-220	Ok. Esp con SLOPE2. Corrisponde al RUN@@. Avvio dell'acquisizione – 180 s dopo l'avvio del paddle.
31 - 100908	60	4	1	1 / 450 / 1 / 1	450	670	-220	Ok. Esp con SLOPE2. Corrisponde al RUN@@. Avvio dell'acquisizione – 120 s dopo l'avvio del paddle.
32 - 110908	60	1	1/5	1 / 1 / 550 / 5	2750	2680	+	Ok. Esp con SLOPE2. Corrisponde al RUN@@.
33 - 110908	30	1	1/5	1 / 1 / 550 / 5	2750	2680	+	Ok. Esp con SLOPE2. Corrisponde al RUN@@. **Attenzione**, l'acqusizione è inavvertitamente ripartita alla fine, sovrascrivendo i primi 21 dati e anche il file txt. Quest'ultimo potrebbe essere sostituito con quello dell'esp precedente (32), i cui tempi devono corrispondere quasi esattamente.
34 - 120908	30	10	2	2 / 450 / 1 / 1	225	268	-43	Esp con CAPE1 (45°). Avvio dell'acquisizione – 45 s dopo l'avvio del paddle. Non c'è separazione.
35 - 120908	30	20	2	2 / 300 / 1 / 1	150	134	+	Esp con CAPE1. Non c'è separazione.
36 - 120908	30	30	3	3 / 270 / 1 / 1	90	89	=	Esp con CAPE1. Non c'è separazione, ma …
37 - 120908	30	40	4	4 / 272 / 1 / 1	68	67	=	Esp con CAPE1. Non c'è separazione, ma alla fine del

9. Organisation of data files:

Everything was perfectly working, there are no remarks concerning the experimental facility. The technical assistance was perfect, as it was in the first experiment done in 2003. The only remark concerns the software that must be used to obtain the velocity vectors from the bitmap images taken from the three digital cameras of the photogrammetry system. Some vectors cannot be obtained from data taken near the coast for reasons that are not yet clear, but the personnel responsible for the measuring system will soon find the solution. As for future developments of our study, now it is probably too early to say. This will appear more clear after a complete processing of the data will be carried out and after the scientific analysis of the results will be performed, but some indication for interesting future developments is outlined at the end of section 3.3.

10. Remarks about the experimental campaign, problems and things to improve:

Window size: x
Viewport size: x